RESEARCH ARTICLE

PALEOCLIMATE

A 550,000-year record of East Asian monsoon rainfall from ^{10}Be in loess

J. Warren Beck,[1,2,3]* Weijian Zhou,[4,5]* Cheng Li,[3] Zhenkun Wu,[3,4] Lara White,[1,3] Feng Xian,[4] Xianghui Kong,[3,4] Zhisheng An[4,6]

Cosmogenic ^{10}Be flux from the atmosphere is a proxy for rainfall. Using this proxy, we derived a 550,000-year-long record of East Asian summer monsoon (EASM) rainfall from Chinese loess. This record is forced at orbital precession frequencies, with higher rainfall observed during Northern Hemisphere summer insolation maxima, although this response is damped during cold interstadials. The ^{10}Be monsoon rainfall proxy is also highly correlated with global ice-volume variations, which differs from Chinese cave δ^{18}O, which is only weakly correlated. We argue that both EASM intensity and Chinese cave δ^{18}O are not governed by high-northern-latitude insolation, as suggested by others, but rather by low-latitude interhemispheric insolation gradients, which may also strongly influence global ice volume via monsoon dynamics.

Chinese speleothem ^{18}O/^{16}O (d^{18}O) isotope ratio records (*1*, *2*), such as the Sanbao Cave record, are clearly linked to the Asian monsoon and provide some of the most high-resolution and best dated records of tropical paleoclimate available. Their extraordinary match with high-latitude (65°N) summer insolation variations suggests a strong coupling with high-latitude climate (*1*); however, the origins of this coupling and of the δ^{18}O variations themselves remains controversial. Wang *et al.* (*2*) originally interpreted Chinese speleothem δ^{18}O as reflecting changes in the mixing ratio of summer versus winter monsoon moisture, each differing in isotopic composition. Subsequent authors have instead suggested that cave δ^{18}O variations were a response to changing upstream Rayleigh fractionation (*3*) or changes in the seasonality of precipitation (*4*), or were a proxy for monsoon intensity (*1*). Still others (*5*) assert that cave δ^{18}O cannot be strictly a proxy for Asian monsoon intensity because according to them, intensity should be phase-lagged from 65°N solar insolation. Thus, it seems the question of what controls cave δ^{18}O remains unclear. Here, we reinterpret these cave records in the context of our ^{10}Be-based East Asian summer monsoon (EASM) rainfall record.

Meteoric ^{10}Be preserved in Pleistocene Chinese loess can be used as a proxy for monsoon paleorainfall. Our sampling site (N34.43°, E107.12°) was chosen in order to study the paleo-EASM, which dominates the regional climate there, providing ~85% of annual rainfall. ^{10}Be is a long-lived cosmogenic radionuclide produced in the atmosphere and does not form gaseous species but instead attaches to atmospheric dust, with deposition mainly mediated by wet precipitation events (*6*, *7*). Its flux can thus be quantitatively linked with rainfall amount, after correcting for geomagnetic field and recycling effects (supplementary materials). Once on the ground, ^{10}Be becomes an immobile oxidized component of the sediments, permitting extraction of a rainfall record with minimal signal loss from diagenesis. Direct comparison with the nearby U/Th–dated Sanbao Cave δ^{18}O record (*1*), which is also reportedly a record of monsoon strength, was made possible by establishing an age model for this record by correlating the large number of similar features observed in both records.

Main findings

Shown in Fig. 1A is our ^{10}Be-proxy rainfall record (Fig. 1A, red curve) compared with the Sanbao δ^{18}O record (Fig. 1A, yellow curve) (*1*). ^{10}Be reveals that EASM rainfall increases during Northern Hemisphere summer insolation maxima and decreases during insolation minima (Fig. 1A, gray dashed curve) (*8*). Fig. 1A shows that EASM rainfall intensity is inversely correlated with speleothem δ^{18}O; however, the scaling deviates during

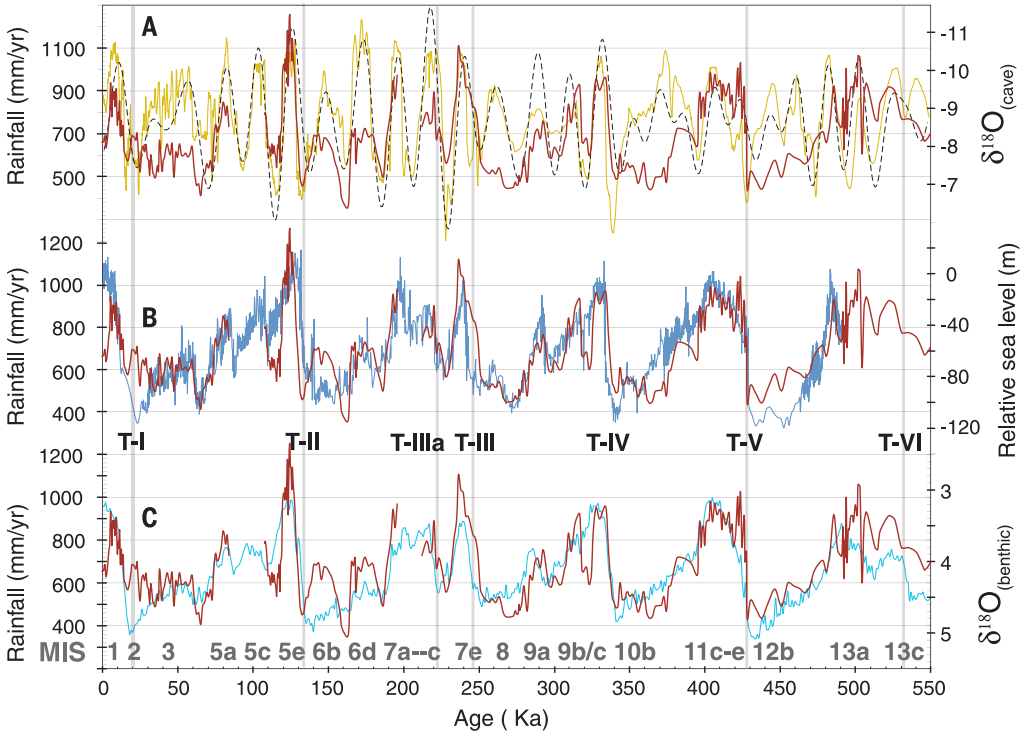

Fig. 1. ^{10}Be-proxy EASM rainfall versus Sanbao Cave d^{18}O, sea level, and benthic foraminiferal d^{18}O records. (**A**) Plot of ^{10}Be-based rainfall (red) versus Sanbao δ^{18}O record (yellow). The δ^{18}O scale is reversed. 65°N June insolation (dashed curve) is also shown (*8*) for reference. Locations of some MIS stages are labeled below (C). MIS stages 5b,c and 7b are missing from our profile (supplementary materials). (**B**) Plot of ^{10}Be-based rainfall (red) versus Red Sea glacio-eustatic sea level curve (blue) relative to modern sea level (*8*), both placed on Sanbao Cave age models. Main glacial terminations (vertical gray bars) are labeled below this figure. (**C**) Plot of ^{10}Be-based rainfall (red) versus LR04 stacked benthic δ^{18}O curve (blue) (*9*).

the cold interstadials of marine isotope (MIS)–3, -6, -8, -10, and -12, where our ^{10}Be-rainfall proxy has lower amplitude than that of the cave isotopes. As a result, we found that only 16.3% of the variance in the ^{10}Be-proxy rainfall record is correlated with the Sanbao record (fig. S1A). Nevertheless, both exhibit strong forcing at precessional periods.

On the other hand, our ^{10}Be-rainfall record is strongly correlated with global ice volume proxies. Shown in Fig. 1B is our record plotted against the Red Sea (RSL) paleosea level reconstruction (*8*), whereas in Fig. 1C we compare it with the LR04 benthic foraminifera δ^{18}O record (*9*). Our rainfall record exhibits very similar structure, with respectively 57 and 51.7% of its variance reflected in each of these two global ice volume proxies (fig. S1, B and C). This suggests that EASM intensity is closely coupled to high-latitude ice volume variations by some mechanism.

Surprisingly, this is not true of the Sanbao Cave δ^{18}O record, which is highly correlated with 65°N summer insolation, but only 10.6% of its variance is correlated with sea-level or global ice volume amplitude (Fig. 2). This creates a conundrum: Although cave δ^{18}O and ^{10}Be monsoon proxies are modestly correlated with each other, the former is highly correlated with insolation but not ice volume, whereas the latter is highly correlated with ice volume but not insolation. The Chinese cave community asserts that its isotope records imply that Asian monsoon intensity is controlled by orbital forcing of high-northern-latitude insolation (*1*, *10*); but if so, how can their proxy for monsoon intensity also be essentially uncorrelated with global ice volume? This seemingly contradicts a principal tenet of the Milankovitch theory, that high-northern-latitude solar insolation controls global ice volume and, through ice albedo feedback, also controls global temperature and, by corollary, tropical monsoon strength. How do we reconcile these two monsoon records, and can we do so without violating the Milankovitch theory?

Interpretation

We suggest that these conflicts may in part be resolved by reinterpreting the cave isotopes as a two-component moisture-mixing proxy instead of monsoon intensity and by recognition that monsoon intensity is determined mainly by low-latitude, not high-latitude, insolation variations. Why, then, are Chinese cave δ^{18}O records so strongly correlated with 65°N summer insolation (Fig. 3A)? The reason is that 65°N insolation exhibits nearly identical phase, net-range, and pattern of variations as those of the low-latitude (30°N to 30°S) June solar insolation gradient (Fig. 3B). This finding partly resolves the conflict between the cave records and Milankovitch theory because a connection with ice volume (and ice albedo) is not required if monsoons are forced from low latitudes. Still, this observation weakens the concept that global climate control emanates principally from high-northern-latitude insolation.

The idea that global climate control should chiefly emanate from low latitudes seems a more natural perspective because the amount of solar energy falling between 30°N and 30°S (that is, the region controlling the monsoons) is more than an order of magnitude larger than that falling above 65°N. Furthermore, the monsoons are the primary agent by which this incident energy is transported aloft or to high latitude, where it can be reradiated to space. When coupled with our observation that the ^{10}Be monsoon intensity proxy is highly correlated with global ice volume, this model leads us to suggest that the monsoons may in fact be an important driver of high-latitude climate, rather than the reverse. This model thus deviates from classical Milankovitch theory, although it retains the idea that orbital forcing of insolation is important.

We argue that it is the low-latitude interhemispheric insolation gradient that controls both EASM intensity and Chinese cave δ^{18}O. We assert that this gradient modulates the pattern of upper-tropospheric outflow from the Asian Monsoons to the North Pacific versus Southern Indian Ocean subtropical highs and in so doing regulates the relative strength of Hadley and Walker circulations in the Indo-Pacific sectors. This in turn influences the relative strength of the Indian summer monsoon (ISM) and Western North Pacific summer monsoon (WNPSM). In this model, Chinese cave isotopes are explained by mixing between ^{18}O-depleted moisture derived from the ISM and relatively ^{18}O-undepleted moisture nominally derived from the WNPSM, both of which contribute to EASM rainfall. ISM moisture is generally more δ^{18}O-depleted than WNPSM-sourced moisture because of rainout during transport across India or from greater interaction with topography of the Tibetan Plateau (TP) before arrival in central China (*11*–*13*). Orbital forcing of the interhemispheric insolation gradient, we argue, results in a higher ISM (δ^{18}O-depleted) moisture fraction during boreal summer precession maxima, and vice versa. When this gradient is large, EASM rainfall amount also increases, although the effect is damped during cold interstadials because of persistent summer snow cover on the TP or orbital modulation of Hadley circulation strength (*14*).

Modern evidence

Modern observations (*15*) do in fact show that it is differential heating between the hemispheres at low latitudes—not high-latitude insolation—that controls tropical monsoon development. Modern observations also show that the Asian monsoon is linked to both meridional Hadley and zonal Walker circulation pathways via monsoon outflow to the southern Indian ocean subtropical high (SISH) and north Pacific subtropical high (NPSH) (*16*–*19*). These two subtropical highs are key elements of Hadley and Walker circulation, in which rising air generated by the tropical monsoons descends in the subtropics. We assert that

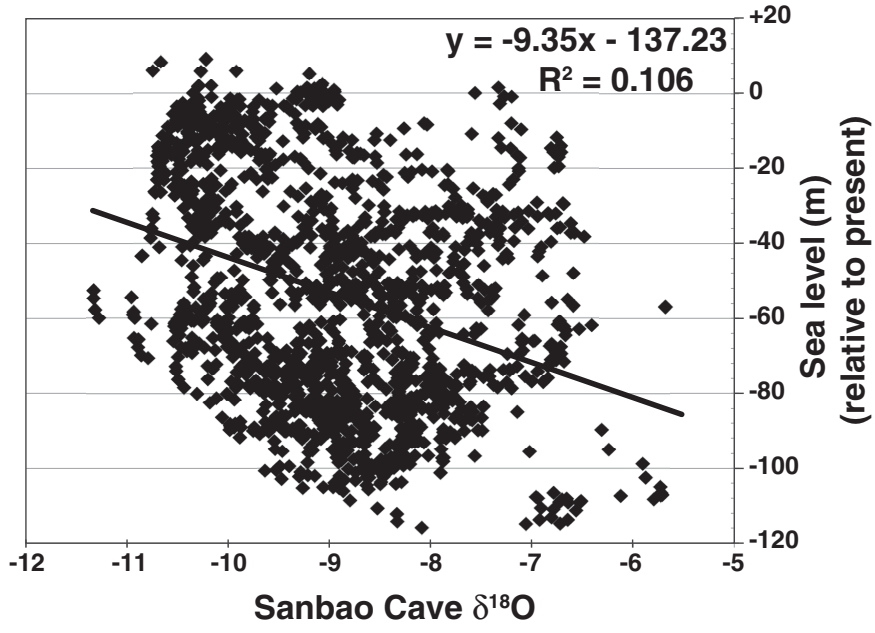

Fig. 2. Correlation between Red Sea glacio-eustatic sea-level reconstruction and Sanbao Cave δ^{18}O, on the same time scale. Only 10.6% of the variance in the cave isotope record is correlated with sea-level changes (*1*, *8*). Because of different sampling intervals, 3000-year smoothing filters have been applied to each record.

[1]Department of Geosciences, University of Arizona, Tucson, AZ 85721, USA. [2]Department of Physics, University of Arizona, Tucson, AZ 85721, USA. [3]NSF–Arizona Accelerator Mass Spectrometry Laboratory, University of Arizona, Tucson, AZ 85721, USA. [4]State Key Laboratory of Loess and Quaternary Geology, Institute of Earth Environment, Chinese Academy of Sciences, Xi'an 710075, China. [5]Qingdao National Laboratory for Marine Science and Technology, Qingdao, China. [6]Institute of Global Environmental Change, Jiaotong University, Xi'an 710061, China.
***Corresponding author. Email: wbeck@physics.arizona.edu (J.W.B.); weijian@loess.llqg.ac.cn (W.Z.)**

orbital forcing of solar insolation can change the ratio of monsoon outflow to these two regions differentially, intensifying the subtropical anticyclone in one sector while weakening it in the other. This in turn modulates the relative strength of the westerlies and trade winds in each sector, with both intensifying in one sector at the expense of the other owing to conservation of angular momentum. But Indian Ocean trade winds couple to the Somali jet (*15*, *19*), which influences ISM strength. North Pacific trade winds, on the other hand, influence the transport of moisture into central China from the WNPSM (*20*). Hence, differentially modulating the trade wind strength in these two sectors affects the mixing ratio of moisture arriving into central China derived from these two monsoons, and this, we believe, is what regulates both cave $\delta^{18}O$ and to a lesser extent EASM intensity, as seen in our ^{10}Be proxy.

That Hadley and Walker circulation in the Indian and North Pacific Ocean sectors are inversely coupled to each other via the pattern of upper-tropospheric monsoon outflow (*16*, *17*) is well documented in the seasonal cycle of atmospheric circulation (*18*, *21*). Observations show that during Boreal summer, the southern Hadley cell strengthens while the northern Hadley cell weakens, mainly in response to intensification of the Asian Monsoons (figs. S2 to S4). These two Hadley cells join at the intertropical convergence zone (ITCZ), which is the rising limb of both cells. During boreal summer, the ITCZ migrates into the Northern Hemisphere (figs. S2 and S3) in response to warmer northern and cooler Southern Hemisphere tropics and subtropics (*22*). Over Asia, this migration is accompanied by northward migration of the upper-tropospheric subtropical zonal westerly jet (*23*, *24*), which moves north of the TP during mid-summer. When it does so, it enhances the Tibetan high circulation pattern, which helps to redirect Asian monsoon outflow to the southern Indian Ocean subtropical high. At the same time, boreal summer heating over the TP (~30°N) drives onshore air mass transport, in which sensible heating from latent heat release in the mid-troposphere strongly drives convective and monsoon general circulation (*15*), producing the world's strongest center of atmospheric circulation. During austral summer, the ITCZ moves back into the Southern Hemisphere and the subtropical jet returns to the south of the TP as the heating centers reverse hemisphere, strengthening the northern and weakening the southern Hadley cells.

Thus, during boreal summer, northward movement of the ITCZ accompanied by heating over the TP strongly enhances northward cross-equatorial atmospheric mass transport in the lower troposphere associated with Hadley circulation. This requires an upper-tropospheric return flow to the Southern Hemisphere for mass balance. When coupled with migration of the subtropical jet, these factors strengthen the overturning circulation in the southern Hadley cell and strengthen both the ISM and WNPSM (*15*, *19*, *21*, *23*). Much of this lower tropospheric cross-equatorial mass flow occurs in the northwest Indian Ocean Somali jet, although a lesser part [~1/3 today (*25*)] occurs in several broad low-level flows north-northeast of Australia and the Bay of Bengal (Fig. 4). These two regions of low-level cross-equatorial flow are part of the reason that the southern Hadley cell completely dominates the global meridional, overturning circulation during boreal summer (*18*, *21*). The other reason is that the southern subtropical highs (~30°S) intensify during boreal summer in response to colder austral winter (June–July–August) temperatures. These southern highs (surface anticyclones) form the descending limb of the southern Hadley cell and are further intensified by strong upper-tropospheric return flows of cold dry air from the Northern Hemisphere that balance the low-level northward monsoonal flows during boreal summer (Fig. 4) (*18*, *19*, *26*). Cold sea surface temperature (SST) in the southern subtropics further enhances these anticyclones by inhibiting evaporation from the sea surface, whereas warmer SST in the northern subtropics allows increased evaporation into the lower to middle troposphere there, weakening those surface highs (*27*).

Thus, the seasonal cycle of differential interhemispheric heating affects where the monsoon outflow goes. Today, although some Asian monsoon outflow falls into the Sahara and Asian interior, the remainder is mainly split between the NPSH and the SISH. Numerous modeling studies (*16*, *17*), reanalysis of modern climate data (*18*, *19*, *21*), and Lagrangian tracers studies of ozone (*28*) all show that this upper-tropospheric monsoon outflow to the Southern Indian Ocean is very strong during boreal summer and weak to the NPSH but reverses during austral summer (fig. S4). These models also show that these strong outflows lead to intensified trade winds in the colder hemisphere (*16*, *29*), where today stronger Indian Ocean trade winds couple directly to the Somali jet, intensifying the Indian Ocean tropical westerlies and the ISM (Fig. 4).

Variations in this cyclic seasonal pattern of monsoon outflow also occur, and reanalysis of modern climate data reveals that these variations are linked to changes in SST. In particular, there is an antiphased SST coupling between the Indian and west central Pacific oceans so that when SST in the Indian ocean is anomalously warm, SST in the west central Pacific is anomalously cool (*30*). This pattern is associated with stronger WNPSM and stronger easterly trade winds in the west Pacific, but weaker tropical westerlies over the Indian ocean and weaker ISM, and vice versa.

More generally, modern climate data show that strong Asian monsoon years are indeed associated with both anomalously strong northward movement of the ITCZ as well as anomalous cooling in the Southern Hemisphere subtropics (*25*, *31*). At the same time, stronger 20th-century ISM correlates with weakening and eastward retreat of the NPSH (*20*), which we argue is linked to weaker monsoonal outflow to the NPSH and stronger outflow to the SISH, as required by mass balance.

Putting this all together, reanalysis of modern climate data shows that strong Asian summer monsoons produce strong upper-tropospheric outflow from the Asian monsoons to the SISH but weak outflow to the NPSH and vise versa. It substantiates the idea that there is an interhemispheric oscillation linking Indian and Pacific ocean SST to trade wind velocity over the Northwest Pacific and Indian ocean sectors, and that the relative trade wind strength regulates the relative flux of moisture in the EASM from these two sectors.

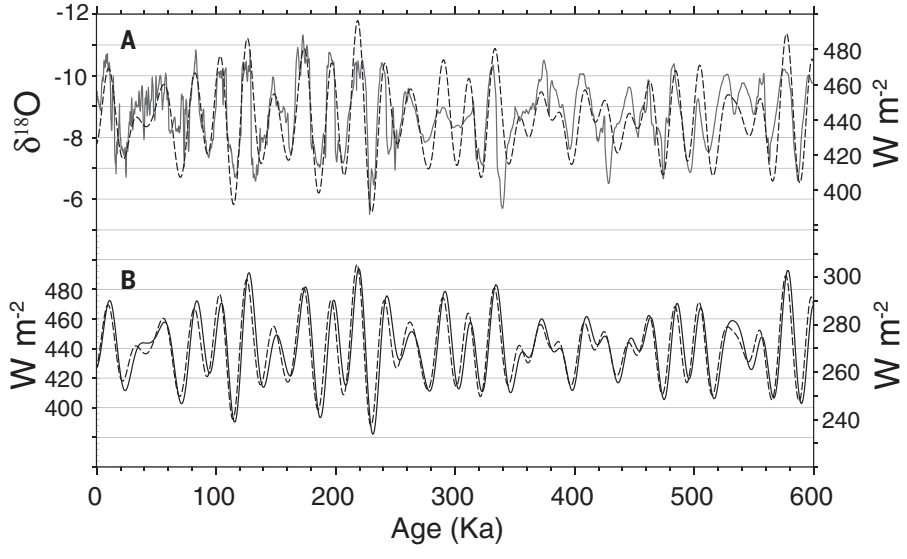

Fig. 3. High-latitude versus low-latitude solar insolation gradient variations compared to Sanbao Cave $d^{18}O$. (**A**) Plot of 65°N June solar insolation (dashed curve) (*39*) versus Sanbao Cave $\delta^{18}O$ record (solid curve) (*1*). The $\delta^{18}O$ scale is reversed. (**B**) Plot of 65°N June solar insolation (dashed curve) versus (30°N to 30°S) June solar insolation difference (solid curve). Visible are the nearly identical pattern and phase and the similar magnitude of changes.

Here lies the linkage between cave $\delta^{18}O$ and the subtropical meridional insolation gradient. Orbitally induced changes of the (June, 30°N to 30°S) subtropical isolation gradient mimic the seasonal cycle of low-latitude insolation variations that drive monsoons. These orbitally induced changes can thus either enhance or diminish this seasonal cycle, depending on the phase. Modeling results (*14*, *32*, *33*) support this idea that orbital-induced changes of the low-latitude interhemispheric insolation gradient do strongly regulate the strength of the winter hemisphere Hadley cell, and that this may work via SST regulation of monsoon outflow to the subtropical highs (*33*) coupled with changes in the mean position of subtropical jet relative to the TP (*23*, *24*). In our mechanism, these changes produce an "intertropical seesaw" between Hadley and Walker circulation that regulates the ratio of EASM moisture derived from the ISM versus WNPSM, modulating Chinese cave $\delta^{18}O$ (Fig. 4). The effect on EASM intensity—as told by the ^{10}Be-proxy—has the same sign and phase but is weaker during cold interstadials because persistent summer snow cover on the TP inhibits onshore monsoon air mass transport and keeps the subtropical westerly jet positioned south of the TP, weakening the Tibetan high.

High- and low-latitude coupling

The observation that variation in the Asian monsoon outflow to the SISH versus NPSH is coupled to trade wind and westerlies velocities in these two sectors reveals another linkage to high-northern-latitude ice volume via the Atlantic meridional overturning circulation (AMOC) (*34*–*38*). AMOC strongly affects the oceanic transport of heat to the high North Atlantic. AMOC in turn is strongly influenced by the Agulhas current leakage of high-salinity water masses from the southern Indian Ocean into the Atlantic. Modulating this source of high-density surface waters profoundly influences North Atlantic Deep Water production—a critical element of AMOC. But Agulhas current leakage is coupled to the strength and position of the SISH (the Mascarene High).

Modern observations between 1993 and 2009 (*34*) demonstrate that intensification of the SISH was indeed accompanied by both southern westerlies and trade wind intensification. The resulting increased wind stress coupling to the sea surface has led to enhanced South Equatorial Current and intensification of the Agulhas western boundary current system in the southwest Indian Ocean (fig. S5). These observations show that both mean kinetic energy and eddy current energy in the Agulhas system increased over this period. Of particular interest is the observation that both westward and southward propagation of mesoscale eddies in the southern Agulhas (32 to 36°S) also increased over this period. Westward propagation of these large eddies into the South Atlantic is the chief mechanism by which the Agulhas leakage occurs. Thus, modern evidence also shows that modulating southern trade wind velocity over the Indian ocean through changing SISH strength could strongly affect AMOC and the transport of heat to the high North Atlantic region.

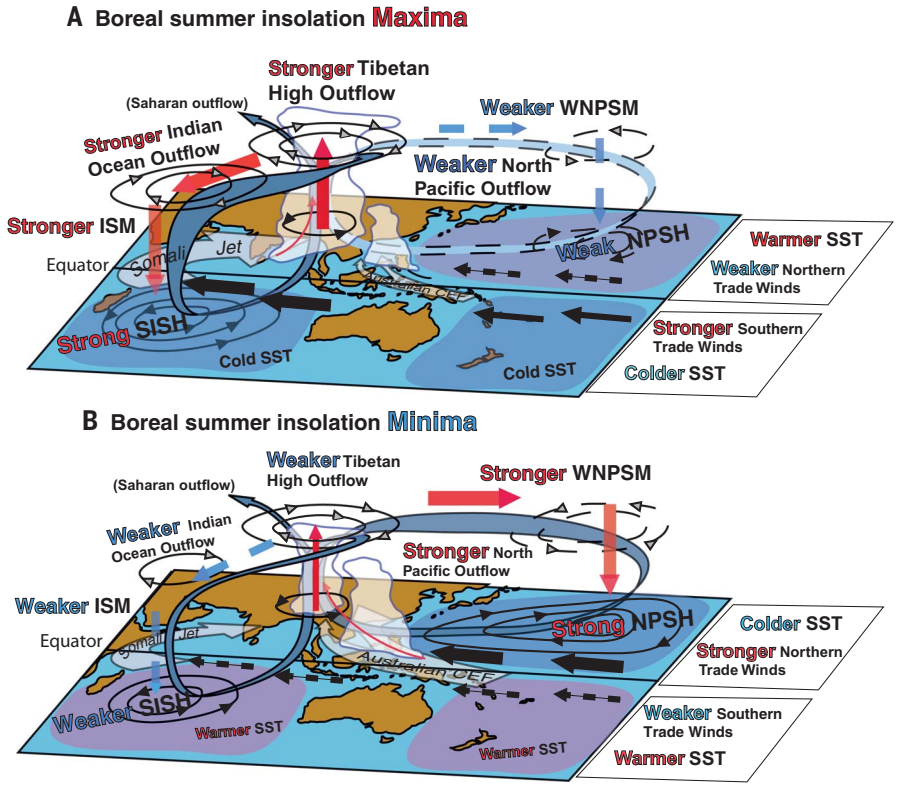

Fig. 4. Intertropical seesaw: Orbitally induced changes in solar insolation mimic the seasonal interhemispheric heating-cooling cycle in the tropics and subtropics. (**A**) During boreal summer insolation maxima, Tibetan high outflow to the SISH is increased in response to two factors: (i) colder SST in the South Indian ocean, which enhances the surface anticyclone there, and (ii) earlier seasonal transition of the upper-tropospheric subtropical zonal westerly jet (*24*, *25*) to the north side of the TP, strengthening the Tibetan high. Both factors enhance Hadley circulation and result in strengthening trade winds and Somali jet in the Indian ocean, strengthening the ISM. At the same time, outflow to the NPSH is reduced in consequence to warmer north Pacific SST, producing weaker northern trade winds and smaller onshore pressure gradient in the North Pacific, weakening the WNPSM. (**B**) During Boreal summer insolation minima, the opposite occurs.

Counteracting effects might also occur, however, because southern trade wind intensification can also lead to increased Agulhas mean velocity, resulting in Agulhas overshoot in the region south of South Africa. In this case, increased Agulhas momentum could carry the current past the zero-wind stress curl latitude into the region dominated by the westerlies, reducing Agulhas leakage and increasing retroflection back into the south Indian Ocean. Instabilities in either one of these two phenomena could produce Dansgaard-Oeschger cycles in the North Atlantic through modulation of AMOC, explaining the close correspondence between Greenland ice core and Chinese cave records on orbital or even suborbital time scales (*1*–*4*). There is evidence for strong increases in Agulhas leakage prefacing each of the past five glacial terminations (*38*), on the basis of the sudden increases of Indian Ocean phytoplankton species in South Atlantic cores that were either concurrent with or occurred just before the ice age terminations.

These observations illustrate how the cave isotope and ^{10}Be rainfall proxy records can be reconciled and show that there are mechanisms by which the Asian monsoon can directly influence high-northern-hemisphere climate, reopening the fundamental paleoclimate question of whether, or to what degree, glacial and interglacial climate is being forced from high versus low latitudes.

REFERENCES AND NOTES

1. H. Cheng *et al.*, *Nature* **534**, 640–646 (2016).
2. Y. J. Wang *et al.*, *Science* **294**, 2345–2348 (2001).
3. D. Yuan *et al.*, *Science* **304**, 575–578 (2004).
4. H. Cheng, A. Sinha, X. Wang, F. Cruz, R. Edwards, *Clim. Dyn.* **39**, 1045–1062 (2012).
5. S. Clemens, W. Prell, Y. Sun, *Paleoceanography* **25**, 1–19 (2010).
6. S. Caillet, P. Arpagaus, F. Monna, J. Dominik, *J. Environ. Radioact.* **53**, 241–256 (2001).
7. W. J. Zhou *et al.*, *Radiocarbon* **49**, 139–160 (2007).
8. K. M. Grant *et al.*, *Nat. Commun.* **5**, 5076 (2014).
9. L. E. Lisiecki, M. E. Raymo, *Paleoceanography* **20**, PA001071 (2005).
10. H. Cheng *et al.*, *Science* **326**, 248–252 (2009).
11. The phasing of cave isotopes in the Himalayas region of northeast India (which are in phase with Chinese lowland cave records, but outside the EASM district) may also be explained by this mechanism. In that region, the westward propagating

moisture vector carries relatively unfractionated moisture in part locally derived from the Bay of Bengal, although its transport is nonetheless still influenced by WNPSM dynamics (*12*).
12. S. Sengupta, A. Sarkar, *Earth Planet. Sci. Lett.* **250**, 511–521 (2006).
13. R. Shukla, B. Huang, *Clim. Dyn.* **46**, 1977–1990 (2016).
14. D. F. Mantsis *et al*., *J. Clim.* **27**, 5504–5516 (2014).
15. P. Webster, in *The Hadley Circulation: Present, Past and Future*, H. F. Diaz, R. S. Bradley, Eds. (Kluwer Academic Publishers, 2005), pp. 9–60.
16. A. E. Gill, *Quat. J. R. Met. Soc.* **106**, 447–462 (1980).
17. F. Liu, B. Wang, *Am. Met. Soc.* **26**, 1791–1806 (2013).
18. J. Schwendike *et al*., *J. Geophys. Res.* **119**, 1322–1339 (2014).
19. J. Walker, S. Bordoni, T. Schneider, *J. Clim.* **28**, 3731–3750 (2015).
20. Y. Huang, H. Wang, K. Fan, Y. Gao, *Clim. Dyn.* **44**, 2035–2047 (2015).
21. I. Dima, J. M. Wallace, I. Kraucunas, *Am. Met. Soc.* **62**, 2499–2513 (2005).
22. G. Basha *et al*., *Remote Sens. Environ.* **163**, 262–269 (2015).
23. J. Chiang *et al*., *Quat. Sci. Rev.* **108**, 111–129 (2014).
24. R. Schiemann, D. Lüthi, C. Schär, *J. Clim.* **22**, 2940–2957 (2009).
25. Y. Zhu, *Adv. Atmos. Sci.* **29**, 509–518 (2012).
26. S.-L. Lee, C. Mechoso, C. Wang, J. D. Neelin, *J. Clim.* **26**, 10193–10204 (2013).
27. T. Shaw, A. Voigt, *Nat. Geosci.* **8**, 560–566 (2015).
28. M. Hitchman, M. Rogal, *J. Geophys. Res.* **115**, D14118 (2010).
29. A. Broccoli, K. Dahl, R. Stouffer, *Geophys. Res. Lett.* **33**, L01702 (2006).
30. J. Cao, S. Gui, Q. Su, Y. Yang, *J. Clim.* **29**, 5027–5040 (2016).
31. C. Li, S. Li, *Am. Met. Soc.* **27**, 3966–3981 (2014).
32. M. Erb, A. Broccoli, A. Clement, *J. Clim.* **26**, 5897–5914 (2013).
33. M. Erb *et al*., *J. Clim.* **28**, 9258–9276 (2015).
34. B. Backeberg, P. Penven, M. Rouault, *Nat. Clim. Chang.* **2**, 608–612 (2012).
35. L. M. Beal, W. P. De Ruijter, A. Biastoch, R. Zahn, SCOR/WCRP/IAPSO Working Group 136, *Nature* **472**, 429–436 (2011).
36. L. Braby *et al*., *Geophys. Res. Lett.* **43**, 8143–8150 (2016).
37. W. Broeker, *Oceanography* **4**, 79–89 (1991).
38. F. J. Peeters *et al*., *Nature* **430**, 661–665 (2004).
39. A. Berger, M. F. Loutre, *Quat. Sci. Rev.* **10**, 297–317 (1991).

ACKNOWLEDGMENTS

This work was jointly supported by the U.S. National Science Foundation through EAR-0908709, EAR-0902633, and EAR-0929458, as well as the Ministry of Science and Technology of China, the National Science Foundations of China, and the Key Research Programs of Frontier Sciences, Chinese Academy of Sciences. We also gratefully acknowledge insightful editorial assistance from J. Russell and P. Goodman, University of Arizona Geosciences Department, and three anonymous reviewers. The data used in this work can be found in the associated supplementary materials.

SUPPLEMENTARY MATERIALS

www.sciencemag.org/content/360/6391/877/suppl/DC1
Materials and Methods
Figs. S1 to S7
Tables S1 and S2
References (*40*–*54*)

15 December 2016; accepted 30 March 2018
10.1126/science.aam5825

Science

A 550,000-year record of East Asian monsoon rainfall from ^{10}Be in loess

J. Warren Beck, Weijian Zhou, Cheng Li, Zhenkun Wu, Lara White, Feng Xian, Xianghui Kong and Zhisheng An

Science **360** (6391), 877-881.
DOI: 10.1126/science.aam5825

Forcing the East Asian summer monsoon

What factors have controlled the intensity of the East Asian summer monsoon over the recent geological past? To answer this key question requires a robust proxy for rainfall amounts. Beck *et al.* measured the beryllium isotopic content of loess from China, from which they reconstructed a 550,000-year-long record of rainfall. Rainfall correlated with orbital precession and global variations in ice volume. This finding suggests that the monsoon is governed by low-latitude interhemispheric gradients in solar radiation levels, rather than by high-northern-latitude solar radiation levels as previously suggested.

Science, this issue p. 877